AGU PUBLICATIONS

Geophysical Research Letters

RESEARCH LETTER
10.1002/2018GL077065

Key Points:
- The frequency and intensity of subdaily precipitation extremes has increased in India
- The contribution from the dynamic scaling is higher than the thermodynamic scaling
- Subdaily precipitation extremes show higher regression slopes (against dew point temperature) than daily regression slopes

Supporting Information:
- Supporting Information S1

Correspondence to:
V. Mishra,
vmishra@iitgn.ac.in

Citation:
Ali, H., & Mishra, V. (2018). Contributions of dynamic and thermodynamic scaling in subdaily precipitation extremes in India. *Geophysical Research Letters*, *45*, 2352–2361. https://doi.org/10.1002/2018GL077065

Received 7 JAN 2018
Accepted 23 FEB 2018
Accepted article online 28 FEB 2018
Published online 14 MAR 2018

Contributions of Dynamic and Thermodynamic Scaling in Subdaily Precipitation Extremes in India

Haider Ali[1] **and Vimal Mishra**[1]

[1]Department of Civil Engineering, Indian Institute of Technology, Gandhinagar, India

Abstract Despite the importance of subdaily precipitation extremes for urban areas, the role of dynamic and thermodynamic scaling in changes in precipitation extremes in India remains poorly constrained. Here we estimate contributions from thermodynamic and dynamic scaling on changes in subdaily precipitation extremes for 23 urban locations in India. Subdaily precipitation extremes have become more intense during the last few decades. Moreover, we find a twofold rise in the frequency of subdaily precipitation extremes during 1979–2015, which is faster than the increase in daily precipitation extremes. The contribution of dynamic scaling in this rise in the frequency and intensity of subdaily precipitation extremes is higher than the thermodynamic scaling. Moreover, half-hourly precipitation extremes show higher contributions from the both thermodynamic (~10%/K) and dynamic (~15%/K) scaling than daily (6%/K and 9%/K, respectively) extremes indicating the role of warming on the rise in the subdaily precipitation extremes in India. Our findings have implications for better understanding the dynamic response of precipitation extremes under the warming climate over India.

Plain Language Summary Understanding the changes in precipitation extremes in urban areas with warming climate can be valuable in mitigating the adverse social and financial consequences. India has witnessed a twofold rise in the frequency of subdaily precipitation extremes during 1979–2015. This increase in the subdaily frequency of extreme precipitation events is higher than the frequency of daily precipitation extremes. Urban areas in India witness flooding due to increasing extreme precipitation events, which caused enormous damage to infrastructure. Despite the increase in subdaily extreme precipitation in India, the contribution of thermodynamic and dynamic scaling remains largely unexplored. We show that subdaily precipitation extremes have substantially larger contribution from thermodynamic and dynamic scaling than that of daily precipitation extremes. We find that subdaily precipitation extremes are more strongly related to changes in variations in the atmospheric motion and increase in vertical velocity than the rise in atmospheric moisture content. Our work will help in understanding the subdaily precipitation extremes in India under the warming climate.

1. Introduction

Urban areas are the centers of population, economic growth, and wealth (Cohen, 2006; Henderson, 2000). Observed climatic extremes have increased in global urban areas resulting in a rise in the frequency of precipitation extremes (PE) (Mishra et al., 2015), which cause flooding, disrupt transportation, damages urban infrastructure, and may result in loss of human lives (Ali & Mishra, 2017; Ali et al., 2014). During the recent past, urban areas in India have witnessed unprecedented PE. For instance, Mumbai observed 940 mm in 18 h in July 2005, which affected about 20 million people and caused deaths of 1,200 people (Gupta & Nair, 2011). More recently, in September 2017, Mumbai experienced another PE (330 mm in a day) that caused flooding and resulted in delayed flights and halted road and rail transportation. Similarly, devastating effects were observed in Chennai due to extreme precipitation (483 mm in 2 days) in November 2015 (Boyaj et al., 2017). Daily PE in India have increased over the last century and are projected to increase further under the warming climate (Ali & Mishra, 2017; Ali et al., 2014; Dash et al., 2009; Roxy et al., 2017; Sen Roy, 2009; Singh et al., 2014; Vinnarasi & Dhanya, 2016; Vittal et al., 2013).

Understanding the changes in PE in urban areas with warming climate can be valuable in mitigating the adverse social and financial consequences (Fildier et al., 2017). Since PE occur when air is close to saturation, the Clausius-Clapeyron (C-C) relationship is used to explain an increase in the observed and projected extreme precipitation with the rise in air temperature (Ali & Mishra, 2017; Lenderink & Van Meijgaard, 2008; Mishra, Smoliak, et al., 2012; Wasko & Sharma, 2015; Wasko et al., 2015, 2016; Westra et al., 2014).

However, in the tropical regions, PE do not increase with the same rate as atmospheric moisture content and deviate from the proposed 7%/K rate (Fildier et al., 2017; O'Gorman & Schneider, 2009; Pall et al., 2007; Pfahl et al., 2017).

Besides atmospheric moisture content, PE are also influenced by the other thermodynamic and dynamic properties such as changes in temperature lapse rate and vertical wind velocities (Pfahl et al., 2017; Sugiyama et al., 2010). Thermodynamic changes are due to the change in atmospheric moisture content and can be estimated by considering the condensation rate for an adiabatically lifted air parcel (Emori & Brown, 2005; Muller et al., 2011; O'Gorman & Schneider, 2009). On the other hand, changes in dynamically induced precipitation are strongly linked to the variations in the atmospheric motion and increase in vertical velocity associated with extreme precipitation events (Muller et al., 2011). Therefore, for the complete understanding of scaling relationship of PE under the warming climate, consideration of both dynamic and thermodynamic scaling is important (O'Gorman, 2015; Pfahl et al., 2017).

Despite the profound implications of PE in urban areas, the response of subdaily PE in India to thermodynamic and dynamic changes remains unexplored. Most of the previous studies focused on daily PE at the regional or global scales (Pfahl et al., 2017; Roxy et al., 2017), while changes in subdaily or hourly PE and the contribution of dynamic and thermodynamic scaling are not well understood. This is important as we hypothesize that the contribution of dynamic and thermodynamic scaling may vary with the duration of PE. Using subdaily data at finer spatial scale (8 km), we estimate changes in the subdaily (half hour to 12 h) and daily (24 h) PE at 23 urban locations in India. Then the contributions of thermodynamic and dynamic scaling on PE are estimated.

2. Data and Methods

The analysis was conducted for 23 urban locations (Ali & Mishra, 2017) where station data (mostly from airports) of daily precipitation and dew point temperature (DPT) are available. We obtained polygons of the urban areas using urban extent map of global cities based on Moderate Resolution Imaging Spectroradiometer 1 km land cover data (Schneider et al., 2009; supporting information Table S1). These locations were selected based on the availability of station-based long-term observations from Global Summary of Day (GSOD, please see Ali & Mishra, 2017, for more details). The data sets used in our study are summarized in Table S2.

Subhourly (30 min) precipitation data were obtained from Climate Prediction Center morphing technique (CMORPH) at 8 km resolution for the period of 1998–2015 (Xie et al., 2017). Xie et al. (2017) reprocessed purely satellite-based CMORPH precipitation estimates using the integral algorithm, which was bias corrected on an 8 km $\times$ 8 km grid over the globe by matching probability density function against Climate Prediction Center daily gauge analysis over the land and Global Precipitation Climatology Project pentad merged analysis over the ocean. The CMORPH algorithm produces precipitation estimates by using both microwave (MW) and infrared (IR) sensors, and this technique is better than the blended infrared and passive microwave (IR-PMW) precipitation estimation, which uses IR-derived precipitation estimates in absence of PMW data (Joyce et al., 2004). Since the long-term subhourly data for India are unavailable, this is probably the best resource that can be used to understand changes and spatial variability (due to its high spatial resolution) in PE at urban locations in India. The other precipitation products were obtained from Multi-Source Weighted-Ensemble Precipitation (MSWEP; 3-hourly; Beck et al.,2017), Tropical Rainfall Measuring Mission (TRMM) 3B42v7 (3-hourly; Huffman et al., 2003; Prakash et al., 2016), Indian Meteorological Department (IMD; daily; Pai et al., 2014, 2015), and GSOD daily station-based observations. The description of these data sets can be found in supporting information and Table S2.

Daily mean air temperature, vertical wind velocity at different vertical pressure levels (1,000–50 hPa; up to the tropospheric level where lapse rate is 2 K/km), and the daily mean surface temperature at 2 m at 0.25° was obtained from European Reanalysis (ERA)-Interim reanalysis (Dee et al., 2011). ERA-Interim reanalysis data are developed by the European Centre for Medium-Range Weather Forecasts which can be downloaded from http://apps.ecmwf.int/datasets/data/interim-full-daily/levtype=pl/ and are available from January 1979 to present (Dee et al., 2011).

We estimated the changes in subdaily and daily extreme precipitation events in 23 urban locations using the station (GSOD) and gridded precipitation data sets (IMD, MSWEP, TRMM, and CMORPH). Mean precipitation

for each urban area was estimated using grids lying within the polygon of an urban area and 95th percentile (of the entire period for rainy days; precipitation ≥ 1 mm) of precipitation was considered as a threshold to estimate the frequency of extreme precipitation. We estimated the number of extreme precipitation events for each location in a year exceeding the 95th percentile threshold. Then, for each year, the annual time series of the frequency of extreme precipitation for all the locations were summed and divided by the total number (23) of urban areas to get an extreme precipitation index (EPI). The pooled analysis provides us the changes in subdaily and daily precipitation for all the 23 stations in India. The trend analysis was performed on the EPI using the nonparametric Mann Kendall (Kendall, 1975; Mann, 1945) and Sen's slope method (Sen, 1968). The statistical significance in trend was estimated at 5% significance level.

2.1. Dynamic and Thermodynamic Scaling

Next, we estimated the full (thermodynamic and dynamic combined) scaling of PE over the selected locations in India. To do this, we first estimated annual maximum precipitation (AMP) for half-hourly data from CMORPH, while AMP for the other durations (1–24 h) was estimated by taking the maxima of moving sum of half-hourly precipitation to longer durations. Then the scaling relationship, as described in Pfahl et al. (2017) and O'Gorman and Schneider (2009), was used. The full scaling can be expressed as

$$P_e \sim -\left\{\omega_e \frac{\mathrm{d}q_s}{\mathrm{d}p}|_{\theta^*}\right\} \tag{1}$$

where P_e, in our case, is AMP or PE (all the events exceeding the threshold in each year) exceeding the 95th percentile for a particular grid and {.} indicates a mass-weighted integral of the product of the corresponding day's upward vertical velocity (ω_e) and vertical derivative of the saturation specific humidity (q_s), at constant saturation equivalent potential temperature (θ^*) over the troposphere as described in Pfahl et al. (2017) and O'Gorman and Schneider (2009). Equation (1) is converted into equality by substituting a constant at the right-hand side of the equation which is termed as precipitation efficiency factor. Moreover, the scaling relationship gives estimates in mm/d which is further multiplied by the precipitation duration to get AMP estimates for a given duration of precipitation. The full scaling here represents precipitation estimates (P_e), while the strength of the relationship between extreme precipitation and DPT is expressed as regression slopes. We have selected all the PE above the 95th percentile to check the robustness of our results obtained for AMP.

For each grid within an urban boundary, AMP (here AMP_{OBS}) was estimated from each precipitation product. Then, for each location, we estimated vertical profiles of daily mean temperature and vertical velocities at each pressure level for the day of AMP. After that, we estimated saturation vapor pressure at each pressure level using the modified Tetens formula (Simmons et al., 1999). Finally, these parameters (vertical profiles of daily mean temperature, saturation vapor pressure, and vertical velocities) were used as input in the scaling relationship to obtain AMP using the full scaling (AMR_{FS}) by integrating vertically over all the pressure levels with the ascent up to troposphere. The troposphere corresponds to the pressure level below 50 hPa with a lapse rate of 2 K km^{-1} (Pfahl et al., 2017). To compute changes in extreme precipitation (AMP or PE: above 95th percentile) with an increase in DPT, linear regression was used as described in Pfahl et al. (2017). We selected local DPT instead of surface air temperature as it is a better predictor of PE under the warming climate in the tropical region (Ali & Mishra, 2017; Lenderink & Van Meijgaard, 2008, 2010).

Likewise, thermodynamic scaling was estimated using equation (1) with a constant ω_e (mean of all the values corresponding to extreme rain events) for the entire period for a particular grid within an urban polygon. To estimate thermodynamic scaling, we did not consider variation in the upward vertical velocity (ω_e) corresponding to extreme precipitation, which was used to estimate the full scaling in equation (1) (Pfahl et al., 2017). The contribution of dynamic scaling was estimated by subtracting the thermodynamic contribution from the changes in full scaling (Pfahl et al., 2017).

3. Results and Discussion

3.1. Observed Changes in Subdaily and Daily PE

First, we estimated changes in the subdaily and daily frequency of extreme precipitation events (EPI) by considering the 95th percentile threshold using data from CMORPH, MSWEP, TRMM, GSOD, and IMD

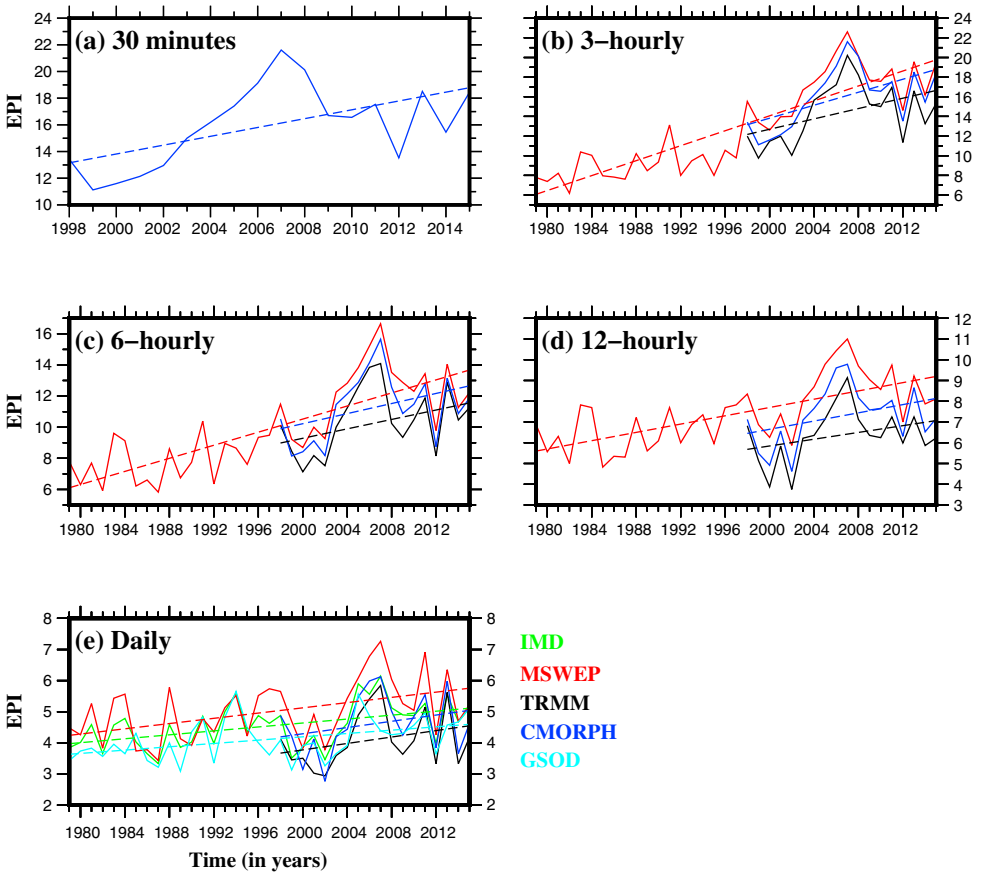

Figure 1. (a–e) Pooled frequency of extreme precipitation events (extreme precipitation index, EPI) per city based on 95th percentile of precipitation, using precipitation data obtained from Indian Meteorological Department (IMD) (green; 1979–2015), Multi-Source Weighted-Ensemble Precipitation (MSWEP) (red; 1979–2015), Global Summary of Day (GSOD) (cyan; 1979–2015), TRMM (black, 1998–2015), and Climate Prediction Center morphing technique (CMORPH) (blue; 1998–2015) for 30 min to daily scale, respectively. The *p* value and *h* value estimated using Mann Kendall test are shown in supporting information Table S3 for all the precipitation data sets at different time scales.

(Figure 1). The period for the trend analysis varied according to the availability of the data from different precipitation products (Table S2). We find a statistically significant ($p < 0.05$) increasing trend in the EPI for most durations (half hour to 24 h), which is consistent for all the precipitation data sets (Figures 1a–1e and Tables S3–S8). Moderate differences in the magnitude of EPI from different precipitation data sets may be due to the differences in the algorithms used in generating these data sets and uncertainties associated with them (Beck et al., 2017; Huffman et al., 2003; Pai et al., 2014; Xie et al., 2017). Overall, we find a twofold increase in the frequency of subdaily extreme precipitation events over the urban locations in India (Figure 1). Further, our results show that the frequency of subdaily PE has increased more rapidly than the daily PE as shown by the long-term data from MSWEP for the period of 1979–2015 (Figure 1). We also estimated trends in daily and subdaily extreme precipitation (mean precipitation intensity) above the 95th percentile of precipitation pooled for all stations. We find statistically significant (*p* value < 0.05) increasing trend in precipitation intensity based on this threshold using MSWEP data for all the durations (supporting information Figure S1 and Tables S9–S14). However, CMORPH and TRMM do not show significant trends, which may be due to the limited period of observations (1998–2015), making the detection of trends difficult as discussed in Coumou and Rahmstorf (2012). We notice a substantial decline in EPI during the 1998–2002 (Figure 1), which can be attributed to strong El Nino of 1997–1998 and a severe drought in 2002. A positive phase of El Niño–Southern Oscillation (ENSO) results in a decline in the summer monsoon rainfall in India (Mishra, Wallace, & Lettenmaier, 2012), while a negative phase of ENSO (La Niña) brings more extreme precipitation events and floods (Krishnamurthy & Goswami, 2000). The 2002 drought during the monsoon season in India was severe with more than 59% reduction in July precipitation (Bhat, 2006), which resulted in a strong decline in EPI (Figure 1).

As in the previous studies (Min et al., 2011), the increasing trends in subdaily and daily EPI at urban locations in India can be explained on the basis of the increase in the moisture holding capacity of the atmosphere under the warming climate (Kharin et al., 2007; Trenberth et al., 2003). The increase in the atmospheric moisture holding capacity results in an increased atmospheric moisture resident time and a shift in precipitation distribution that causes more intense and frequent PE (Pendergrass & Hartmann, 2014; Stephens & Hu, 2010). While there are few studies related to subdaily PE in urban areas in India (Ali et al., 2014; Ali & Mishra, 2017; Sen Roy, 2009), most of the previous studies highlight the role of climate warming on daily extreme precipitation events. For instance, Goswami et al. (2006) reported an increasing magnitude and the frequency of extreme precipitation events over central India in response to climate warming. A similar increase in widespread daily extreme precipitation events is reported in Roxy et al. (2017). Moreover, increase in the land-sea thermal contrast and an increased moisture transport from the Indian Ocean may also intensify PE in India (Mondal & Mujumdar, 2016). A few other studies have attributed an increase in PE to urbanization (Kishtawal et al., 2010; Vittal et al., 2013), while Ali et al. (2014) did not find any significant contribution of urbanization on PE using TRMM data.

Interestingly, our findings show that the frequency of subdaily PE have increased about twofold between 1979 and 2015, and this rate is faster than the increase in the frequency of daily PE. This aspect (difference in trends of subdaily and daily extremes) of PE remains largely neglected in previous studies over India. The faster rise in the frequency of subdaily PE has implications for small catchments and in particular for urban areas that have a large fraction of impervious surface. The scaling relationship between PE and air temperature shows that subdaily PE are more sensitive to warming than daily extremes (Ali & Mishra, 2017; Lenderink & Van Meijgaard, 2008). However, most of the previous studies ignore the different contributions of dynamics and thermodynamics in changes to subdaily PE in India.

3.2. Evaluation of the Full Scaling Against Observed PE

We next analyzed governing mechanisms of increased subdaily PE in 23 urban locations in India (supportinf information Figure S2a and Table S1). We evaluated estimates of AMP using the full scaling (AMP_{FS}) as shown in equation (1) against the estimates of AMP from the CMORPH (AMP_{OBS}) data. We estimated bias (%) in AMP_{FS} against AMP_{OBS} (Figure S2). We find that the full scaling (AMP_{FS}) obtained using the scaling relationship (equation (1)) (considering precipitation efficiency factor equal to 1) is comparable (bias less than 8%) to AMP_{OBS} (Figures S2b–S2g). Scaling relationship was also evaluated for individual stations located in the diverse climate regions in India, which show the consistent results for both AMP_{OBS} and AMP_{FS} (Figure S3). Lenderink and Fowler (2017) argued that since extreme precipitation events vary in space and time, the atmospheric processes resulting in extreme precipitation can be centered over a smaller geographical region. However, most of the short- or long-duration extreme precipitation events occur during the monsoon season in India; therefore, atmospheric processes related to these extreme events can stay for a long duration and over a large area. To evaluate this, we analyzed diurnal variation in vertical velocity at 10 m height using 6-hourly data from ERA-Interim reanalysis at a few locations. Our result shows that vertical velocity remains stable during the day of extreme precipitation indicating similar values of vertical velocity for short and long-duration PE (Figure S4). We find that the scaling relationship slightly underestimates AMP_{FS}, which can be attributed to the constant value (equal to 1) of the precipitation efficiency factor (Pfahl et al., 2017). We also find that the bias between AMP_{FS} and AMP_{OBS} varies within the urban areas. Urban areas located in western India and on the western coast of peninsular India show a higher variability in bias (coefficient of variation = 0.5) than the other urban areas (Figure S2).

We compared the regression slopes estimated using the linear regression between AMP_{FS} and AMP_{OBS} and DPT (Figure 2). This comparison was used as an additional measure (other than the bias (Figure S2) to show the effectiveness of the full scaling to estimate extreme precipitation amounts using the atmospheric variables expressed in the equation (1). We find that regression slopes for AMP_{FS} and AMP_{OBS} are largely similar, with moderate underestimation for AMP_{FS} (Figures 2 and S5). Apart from AMP, we also estimated regression slopes using all the extreme precipitation events exceeding 95th percentile (PE) in each year to evaluate the robustness in our scaling results based on regression (Figure S6). The results are found to be similar using AMP and PE (Figures 2 and S6). Our results show that subdaily PE are more sensitive to rise in DPT than daily PE (Figure 2). Moreover, half-hourly PE show the highest regression slopes for AMP_{FS} and AMP_{OBS}. We find that median regression slopes for AMP_{FS} and AMP_{OBS} for all 23 urban locations are higher than 20%/K

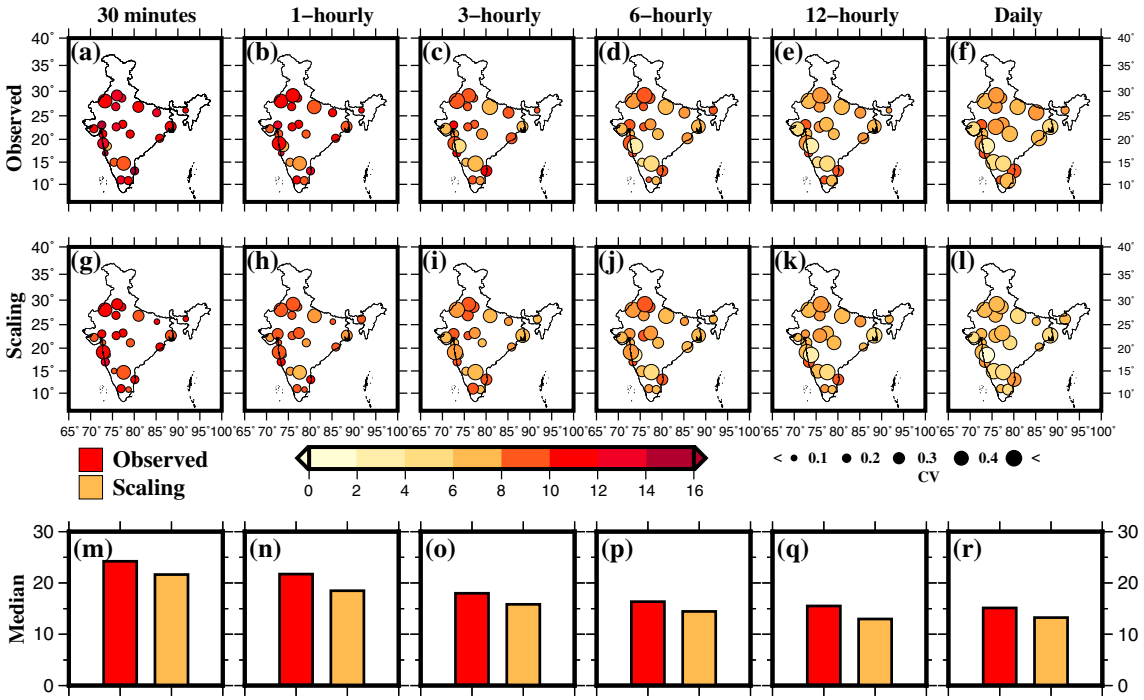

Figure 2. (a–f) Percentage change (regression slopes; in $\%K^{-1}$) in mean annual maximum precipitation (AMP_{OBS}) with respect to per Kelvin (K) increase in dew point temperature obtained using linear regression for the period 1998–2015, using Climate Prediction Center morphing technique data for 30 min to daily scale, respectively, for the selected 23 cities, (g–l) same as (a)–(f) but using AMP_{FS} estimates obtained using scaling relationship, and (m–r) median regression slopes in mean AMP_{OBS} (red) and AMP_{FS} (orange) against dew point temperature. The different size of the circle shows the value of the coefficient of variation in changes in AMP within all grids in a particular urban polygon.

indicating a higher sensitivity of subhourly (half hour to 3 h) than daily (less than 15%/K) PE to rise in DPT (Figure 2).

Since, estimated regression slopes may include long- and short-term variability, we estimated percentage increase in AMP with respect to increase in DPT (%/K) using long-term trends in AMP (AMP_{OBS} and AMP_{FS} from CMORPH) and DPT (O'Gorman, 2012). The ratio of trends in AMP and DPT (median for all cities) are approximately 4%/K lower than our regression estimates (Figure S7). Moreover, estimates of the regression slopes were consistent with the other precipitation products (TRMM, MSWEP, IMD, and GSOD) indicating a higher sensitivity of half-hourly PE in India (Figures S8 and S9). These results highlight that the estimates of AMP and regression slopes from the full scaling are consistent with the estimates from CMORPH and the other data set.

3.3. Thermodynamic and Dynamic Scaling Response to DPT

Next, we separated the contributions from the dynamic and thermodynamic scaling (using the full scaling) on subdaily to daily PE (Figure 3). We estimated thermodynamic scaling using equation (1) while keeping vertical velocity (ω_e) constant. Regression slopes (% change in AMP/K or PE/K) were estimated from the thermodynamic and dynamic scaling for the period 1998–2015 (Figure 3). We find that the majority of urban areas show regression slopes higher than C-C scaling (higher than 7%/K) for both thermodynamic and dynamic scaling for the subdaily PE (Figures 3a–3k). Moreover, the regression slopes are higher (difference up to 5%) for the dynamic scaling as compared to the thermodynamic scaling, which increases from daily to subdaily scales. Half-hourly PE show higher contributions from both thermodynamic (~10%/K) and dynamic (~15%/K) scaling than daily (6 and 9%/K, respectively) extremes. Variation in regression slopes within the urban areas was estimated using the coefficient of variation that ranged from 0.1 to 0.5 and increases with the precipitation duration (Figure 3).

The difference in the thermodynamic and dynamic contribution was estimated for the other precipitation products (TRMM, MSWEP, IMD, and GSOD) based on the timing of PE for 3–24 h duration, and results are consistent with CMORPH (Figure S10). Additionally, we used PE_{FS} above 95th percentile and regression slopes for

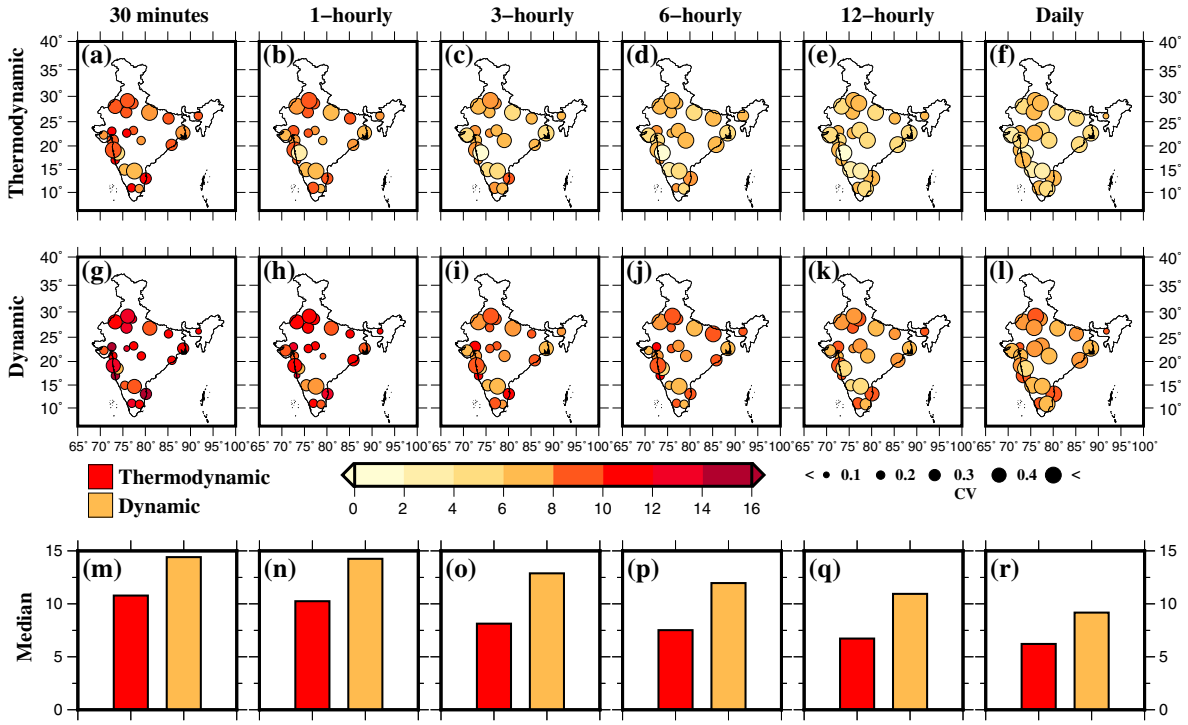

Figure 3. (a–f) Percentage changes (regression slopes; in $\%K^{-1}$) in mean annual maximum precipitation from thermodynamic scaling with respect to per Kelvin (K) increase in dew point temperature (DPT) obtained using linear regression for the period 1998–2015 using Climate Prediction Center morphing technique data for 30 min to daily scale for the selected 23 cities, (g–l) same as (a)–(f) but using AMP obtained from dynamic scaling, and (m–r) median percentage changes in AMP from thermodynamic scaling (red) and dynamic scaling (orange) with DPT. Dynamic scaling was calculated as full scaling minus thermodynamic scaling. The different size of circles shows the value of coefficient of variation in percentage changes in AMP with increase in DPT within all grids in a particular city.

dynamic and thermodynamic scaling for durations half to 24 h were estimated (Figures S11–12). Results for AMP and PE are consistently showing a robust contribution from dynamic and thermodynamic scaling for subdaily to daily PE over India (Figure 4). Pfahl et al. (2017) used ERA-Interim reanalysis and Global Precipitation Climatology Project estimates to check consistencies in scaling results against Coupled Model

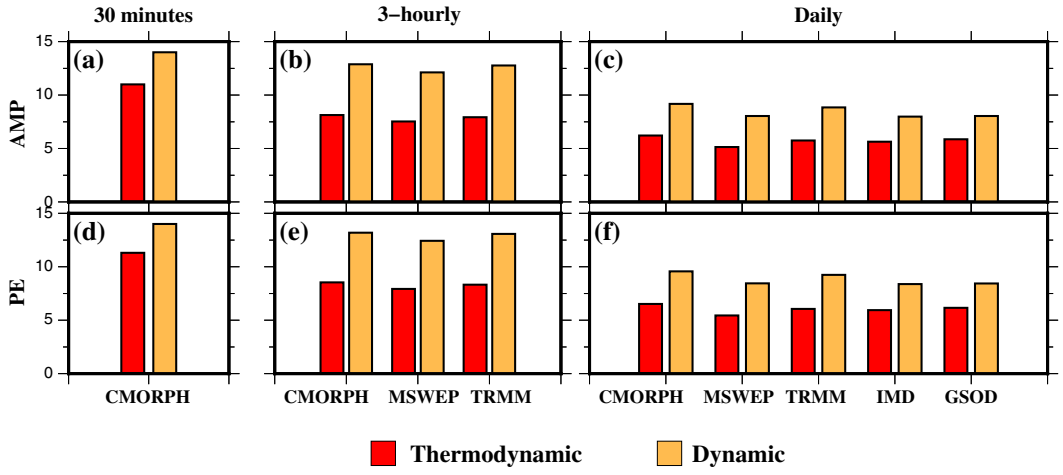

Figure 4. Median percentage changes (regression slopes; in %/K) in annual maximum precipitation (AMP) from thermodynamic scaling (red) and dynamic scaling (orange) against dew point temperature using (a) 30 min precipitation data from Climate Prediction Center morphing technique (CMORPH) (1998–2015), (b) 3-hourly precipitation data from CMORPH (1998–2015), Multi-Source Weighted-Ensemble Precipitation (MSWEP) (1979–2015), and TRMM (1998–2015), respectively, (c) daily precipitation data from CMORPH (1998–2015), MSWEP (1979–2015), TRMM (1998–2015), Indian Meteorological Department (IMD) (1979–2015), and Global Summary of Day (GSOD) (1979–2015), respectively, and (d–f) same as (a)–(c), respectively, but for extreme precipitation (PE) based on 95th percentile of precipitation. Dynamic scaling was calculated as full scaling minus thermodynamic scaling.

Intercomparison Project Phase 5 (CMIP5) models simulations. Our results showing the differences in the dynamic and thermodynamic scaling (for daily durations) are consistent with the findings of Pfahl et al. (2017), suggesting that the dynamic contribution amplifies extreme precipitation over the Indian monsoon region.

There is a linkage between large-scale vertical velocities and subdaily PE; vertical velocities which are associated with large-scale atmospheric conditions, substantially converge moist air which causes intense precipitation events (Lenderink et al., 2017; Lenderink & Attema, 2015). The relatively higher dynamic contribution as compared to thermodynamic contribution may be because of the increase in vertical wind motion which enhances PE (Lau & Kim, 2015; Liu et al., 2009; Muller et al., 2011; O'Gorman & Schneider, 2009; Pfahl et al., 2017). Moreover, the dynamical amplification of extreme precipitation in India can be explained by the dynamic changes of the mesoscale monsoon depressions representing almost all extreme events, which originate on warm waters of Bay of Bengal and move along the monsoon trough (Pfahl et al., 2017; Roxy et al., 2017; Turner & Annamalai, 2012).

4. Conclusions

We evaluated changes in the frequency and mean intensity of subdaily and daily extreme precipitation events over 23 urban locations in India using precipitation data from CMORPH, MSWEP, TRMM, IMD, and GSOD. We observed a statistically significant (p value <0.05) increase in the frequency and intensity of subdaily and daily PE over the period of 1979–2015. The frequency of subdaily PE has increased more rapidly than the daily PE and has increased about twofold in the last three decades. The increase in the frequency of subdaily and daily PE was consistent in all data sets (CMORPH, MSWEP, TRMM, IMD, and GSOD).

We used the full scaling to evaluate the linkage between the increases in subdaily PE with the warming climate. The contribution from the dynamic and thermodynamic scaling on subdaily PE at urban locations was estimated. The full scaling based on saturated vapor pressure and vertical velocity satisfactorily estimates PE (AMP and PE) with minimal (up to 8%) bias against the estimates from CMORPH. Moreover, the regression slopes estimated using the PE from the full scaling and DPT were comparable to the regression slopes estimated using the observed data from CMORPH indicating the effectiveness of the full scaling.

Dynamic scaling shows higher regression slopes as compared to thermodynamic scaling (differences up to 5%). Half-hourly PE show higher contributions from the both thermodynamic (~10%/K) and dynamic (~15%/K) scaling than daily (6 and 9%/K, respectively) extremes. This could be due to the excess latent heat released due to convective nature of precipitation received in the majority of urban areas (Ali & Mishra, 2017). This indicates the importance of dynamic scaling in the sensitivity of subdaily PE over India. The findings reported in this study have implications for better understanding the response of PE under the warming climate over India. Moreover, the higher sensitivity of half-hourly PE further suggests that the short-duration PE, which are more relevant to urban stormwater designs, may increase with even faster rates that have been previously reported.

Acknowledgments
Authors would like to thank Paul O'Gorman for his suggestions and two reviewers for their insightful comments. Authors acknowledge data availability from CMORPH, MSWEP, TRMM, IMD, and ERA-Interim. All the data sets used in this study are publically available. The first author acknowledges the funding from Ministry of Human Resources Development (MHRD). The work was partially supported by the BELMONT forum grant to the second author.

References

Ali, H., & Mishra, V. (2017). Contrasting response of precipitation extremes to increase in surface air and dewpoint temperatures at urban locations in India. *Scientific Reports*, *7*(1), 1228. https://doi.org/10.1038/s41598-017-01306-1

Ali, H., Mishra, V., & Pai, D. S. (2014). Observed and projected urban extreme precipitation events in India. *Journal of Geophysical Research: Atmospheres*, *119*, 12,621–12,641. https://doi.org/10.1002/2014JD022264

Beck, H. E., van Dijk, A. I., Levizzani, V., Schellekens, J., Miralles, D. G., Martens, B., & de Roo, A. (2017). MSWEP: 3-hourly 0.25 global gridded precipitation (1979–2015) by merging gauge, satellite, and reanalysis data. *Hydrology and Earth System Sciences*, *21*(1), 589–615. https://doi.org/10.5194/hess-21-589-2017

Bhat, G. S. (2006). The Indian drought of 2002—A sub-seasonal phenomenon? *Quarterly Journal of the Royal Meteorological Society*, *132*(621), 2583–2602. https://doi.org/10.1256/qj.05.13

Boyaj, A., Ashok, K., Ghosh, S., Devanand, A., & Dandu, G. (2017). The Chennai extreme precipitation event in 2015: The Bay of Bengal connection. *Climate Dynamics*, 1–13.

Cohen, B. (2006). Urbanization in developing countries: Current trends, future projections, and key challenges for sustainability. *Technology in Society*, *28*(1-2), 63–80. https://doi.org/10.1016/j.techsoc.2005.10.005

Coumou, D., & Rahmstorf, S. (2012). A decade of weather extremes. *Nature Climate Change*, *2*(7), 491–496.

Dash, S. K., Kulkarni, M. A., Mohanty, U. C., & Prasad, K. (2009). Changes in the characteristics of rain events in India. *Journal of Geophysical Research*, *114*, D10109. https://doi.org/10.1029/2008JD010572

Dee, D. P., Uppala, S. M., Simmons, A. J., Berrisford, P., Poli, P., Kobayashi, S., & Bechtold, P. (2011). The ERA-interim reanalysis: Configuration and performance of the data assimilation system. *Quarterly Journal of the Royal Meteorological Society*, *137*(656), 553–597. https://doi.org/10.1002/qj.828

Emori, S., & Brown, S. J. (2005). Dynamic and thermodynamic changes in mean and extreme precipitation under changed climate. *Geophysical Research Letters*, *32*, L17706. https://doi.org/10.1029/2005GL023272

Fildier, B., Parishani, H., & Collins, W. D. (2017). Simultaneous characterization of mesoscale and convective-scale tropical precipitation extremes and their dynamical and thermodynamic modes of change. *Journal of Advances in Modeling Earth Systems*, *9*(5), 2103–2119. https://doi.org/10.1002/2017MS001033

Goswami, B. N., Venugopal, V., Sengupta, D., Madhusoodanan, M. S., & Xavier, P. K. (2006). Increasing trend of extreme rain events over India in a warming environment. *Science*, *314*(5804), 1442–1445. https://doi.org/10.1126/science.1132027

Gupta, A. K., & Nair, S. S. (2011). Urban floods in Bangalore and Chennai: Risk management challenges and lessons for sustainable urban ecology. *Current Science*, *100*, 1638–1645.

Henderson, J. V. (2000). *The effects of urban concentration on economic growth (No. w7503)*. Cambridge, MA: National Bureau of Economic Research. https://doi.org/10.3386/w7503

Huffman, G. J., Adler, R. F., Stocker, E. F., Bolvin, D. T., & Nelkin, E. J. (2003). Analysis of TRMM 3-hourly multi-satellite precipitation estimates computed in both real and post-real time. In *12th Conference on Satellite Meteorology and Oceanography*.

Joyce, R. J., Janowiak, J. E., Arkin, P. A., & Xie, P. (2004). CMORPH: A method that produces global precipitation estimates from passive microwave and infrared data at high spatial and temporal resolution. *Journal of Hydrometeorology*, *5*(3), 487–503. https://doi.org/10.1175/1525-7541(2004)005%3C0487:CAMTPG%3E2.0.CO;2

Kendall, M. G. (1975). *Rank correlation methods*. New York: Oxford University Press.

Kharin, V. V., Zwiers, F. W., Zhang, X., & Hegerl, G. C. (2007). Changes in temperature and precipitation extremes in the IPCC ensemble of global coupled model simulations. *Journal of Climate*, *20*(8), 1419–1444. https://doi.org/10.1175/JCLI4066.1

Kishtawal, C. M., Niyogi, D., Tewari, M., Pielke, R. A., & Shepherd, J. M. (2010). Urbanization signature in the observed heavy precipitation climatology over India. *International Journal of Climatology*, *30*(13), 1908–1916. https://doi.org/10.1002/joc.2044

Krishnamurthy, V., & Goswami, B. N. (2000). Indian monsoon–ENSO relationship on interdecadal timescale. *Journal of Climate*, *13*(3), 579–595. https://doi.org/10.1175/1520-0442(2000)013%3C0579:IMEROI%3E2.0.CO;2

Lau, W. K., & Kim, K.-M. (2015). Robust Hadley circulation changes and increasing global dryness due to CO_2 warming from CMIP5 model projections. *Proceedings of the National Academy of Sciences*, *112*(12), 3630–3635.

Lenderink, G., & Attema, J. (2015). A simple scaling approach to produce climates cenarios of local precipitation extremes for the Netherlands. *Environmental Research Letters*, *10*(8), 085001. https://doi.org/10.1088/1748-9326/10/8/085001

Lenderink, G., Barbero, R., Loriaux, J. M., & Fowler, H. J. (2017). Super-Clausius–Clapeyron scaling of extreme hourly convective precipitation and its relation to large-scale atmospheric conditions. *Journal of Climate*, *30*(15), 6037–6052. https://doi.org/10.1175/JCLI-D-160808.1

Lenderink, G., & Fowler, H. J. (2017). Hydroclimate: Understanding rainfall extremes. *Nature Climate Change*, *7*(6), 391–393. https://doi.org/10.1038/nclimate3305

Lenderink, G., & Van Meijgaard, E. (2008). Increase in hourly precipitation extremes beyond expectations from temperature changes. *Nature Geoscience*, *1*(8), 511–514. https://doi.org/10.1038/ngeo262

Lenderink, G., & Van Meijgaard, E. (2010). Linking increases in hourly precipitation extremes to atmospheric temperature and moisture changes. *Environmental Research Letters*, *5*(2), 025208. https://doi.org/10.1088/1748-9326/5/2/025208

Liu, S. C., Fu, C., Shiu, C. J., Chen, J. P., & Wu, F. (2009). Temperature dependence of global precipitation extremes. *Geophysical Research Letters*, *36*, L17702. https://doi.org/10.1029/2009GL040218

Mann, H. B. (1945). Nonparametric tests against trend. *Econometrica: Journal of the Econometric Society*, *13*(3), 245–259. https://doi.org/10.2307/1907187

Min, S.-K., Zhang, X., Zwiers, F. W., & Hegerl, G. C. (2011). Human contribution to more-intense precipitation extremes. *Nature*, *470*(7334), 378–381. https://doi.org/10.1038/nature09763

Mishra, V., Ganguly, A. R., Nijssen, B., & Lettenmaier, D. P. (2015). Changes in observed climate extremes in global urban areas. *Environmental Research Letters*, *10*(2), 024005. https://doi.org/10.1088/1748-9326/10/2/024005

Mishra, V., Smoliak, B. V., Lettenmaier, D. P., & Wallace, J. M. (2012). A prominent pattern of year-to-year variability in Indian Summer Monsoon Rainfall. *Proceedings of the National Academy of Sciences*, *109*(19), 7213–7217. https://doi.org/10.1073/pnas.1119150109

Mishra, V., Wallace, J. M., & Lettenmaier, D. P. (2012). Relationship between hourly extreme precipitation and local air temperature in the United States. *Geophysical Research Letters*, *39*, L16403. https://doi.org/10.1029/2012GL052790

Mondal, A., & Mujumdar, P. P. (2016). Detection of change in flood return levels under global warming. *Journal of Hydrologic Engineering*, *21*(8), 04016021. https://doi.org/10.1061/(ASCE)HE.1943-5584.0001326

Muller, C. J., O'Gorman, P. A., & Back, L. E. (2011). Intensification of precipitation extremes with warming in a cloud-resolving model. *Journal of Climate*, *24*(11), 2784–2800. https://doi.org/10.1175/2011JCLI3876.1

O'Gorman, P. A. (2012). Sensitivity of tropical precipitation extremes to climate change. *Nature Geoscience*, *5*(10), 697–700. https://doi.org/10.1038/ngeo1568

O'Gorman, P. A. (2015). Precipitation extremes under climate change. *Current Climate Change Reports*, *1*(2), 49–59. https://doi.org/10.1007/s40641-015-0009-3

O'Gorman, P. A., & Schneider, T. (2009). The physical basis for increases in precipitation extremes in simulations of 21st-century climate change. *Proceedings of the National Academy of Sciences*, *106*(35), 14,773–14,777. https://doi.org/10.1073/pnas.0907610106

Pai, D. S., Sridhar, L., Badwaik, M. R., & Rajeevan, M. (2015). Analysis of the daily precipitation events over India using a new long period (1901–2010) high resolution (0.25×0.25) gridded precipitation data set. *Climate Dynamics*, *45*(3–4), 755–776. https://doi.org/10.1007/s00382-014-2307-1

Pai, D. S., Sridhar, L., Rajeevan, M., Sreejith, O. P., Satbhai, N. S., & Mukhopadhyay, B. (2014). Development of a new high spatial resolution (0.25×0.25) long period (1901–2010) daily gridded precipitation data set over India and its comparison with existing data sets over the region. *Mausam*, *65*(1), 1–18.

Pall, P., Allen, M. R., & Stone, D. A. (2007). Testing the Clausius–Clapeyron constraint on changes in extreme precipitation under CO2 warming. *Climate Dynamics*, *28*(4), 351–363. https://doi.org/10.1007/s00382-006-0180-2

Pendergrass, A. G., & Hartmann, D. L. (2014). Changes in the distribution of rain frequency and intensity in response to global warming. *Journal of Climate*, *27*(22), 8372–8383. https://doi.org/10.1175/JCLI-D-14-00183.1

Pfahl, S., O'Gorman, P. A., & Fischer, E. M. (2017). Understanding the regional pattern of projected future changes in extreme precipitation. *Nature Climate Change*, *7*(6), 423–427. https://doi.org/10.1038/nclimate3287

Prakash, S., Mitra, A. K., Pai, D. S., & AghaKouchak, A. (2016). From TRMM to GPM: How well can heavy precipitation be detected from space? *Advances in Water Resources*, *88*, 1–7. https://doi.org/10.1016/j.advwatres.2015.11.008

Roxy, M. K., Ghosh, S., Pathak, A., Athulya, R., Mujumdar, M., Murtugudde, R., et al. (2017). A threefold rise in widespread extreme rain events over central India. *Nature Communications*, *8*(1), 708. https://doi.org/10.1038/s41467-017-00744-9

Schneider, A., Friedl, M. A., & Potere, D. (2009). A new map of global urban extent from MODIS satellite data. *Environmental Research Letters*, *4*(4), 044003. https://doi.org/10.1088/1748-9326/4/4/044003

Sen, P. K. (1968). Estimates of the regression coefficient based on Kendall's tau. *Journal of the American Statistical Association*, *63*(324), 1379–1389. https://doi.org/10.1080/01621459.1968.10480934

Sen Roy, S. (2009). A spatial analysis of extreme hourly precipitation patterns in India. *International Journal of Climatology*, *29*(3), 345–355. https://doi.org/10.1002/joc.1763

Simmons, A. J., Untch, A., Jakob, C., Kaallberg, P., & Unden, P. (1999). Stratospheric water vapour and tropical tropopause temperatures in ECMWF analyses and multi-year simulations. *Quarterly Journal of the Royal Meteorological Society*, *125*(553), 353–386. https://doi.org/10.1002/qj.49712555318

Singh, D., Tsiang, M., Rajaratnam, B., & Diffenbaugh, N. S. (2014). Observed changes in extreme wet and dry spells during the South Asian summer monsoon season. *Nature Climate Change*, *4*(6), 456–461. https://doi.org/10.1038/nclimate2208

Stephens, G. L., & Hu, Y. (2010). Are climate-related changes to the character of global-mean precipitation predictable? *Environmental Research Letters*, *5*(2), 025209. https://doi.org/10.1088/1748-9326/5/2/025209

Sugiyama, M., Shiogama, H., & Emori, S. (2010). Precipitation extreme changes exceeding moisture content increases in MIROC and IPCC climate models. *Proceedings of the National Academy of Sciences*, *107*(2), 571–575. https://doi.org/10.1073/pnas.0903186107

Trenberth, K. E., Dai, A., Rasmussen, R. M., & Parsons, D. B. (2003). The changing character of precipitation. *Bulletin of the American Meteorological Society*, *84*(9), 1205–1218. https://doi.org/10.1175/BAMS-84-9-1205

Turner, A. G., & Annamalai, H. (2012). Climate change and the South Asian summer monsoon. *Nature Climate Change*, *2*(8), 587–595. https://doi.org/10.1038/nclimate1495

Vinnarasi, R., & Dhanya, C. T. (2016). Changing characteristics of extreme wet and dry spells of Indian monsoon precipitation. *Journal of Geophysical Research: Atmospheres*, *121*, 2146–2160. https://doi.org/10.1002/2015JD024310

Vittal, H., Karmakar, S., & Ghosh, S. (2013). Diametric changes in trends and patterns of extreme precipitation over India from pre-1950 to post-1950. *Geophysical Research Letters*, *40*, 3253–3258. https://doi.org/10.1002/grl.50631

Wasko, C., & Sharma, A. (2015). Steeper temporal distribution of rain intensity at higher temperatures within Australian storms. *Nature Geoscience*, *8*(7), 527–529. https://doi.org/10.1038/ngeo2456

Wasko, C., Sharma, A., & Johnson, F. (2015). Does storm duration modulate the extreme precipitation-temperature scaling relationship? *Geophysical Research Letters*, *42*, 8783–8790. https://doi.org/10.1002/2015GL066274

Wasko, C., Sharma, A., & Westra, S. (2016). Reduced spatial extent of extreme storms at higher temperatures. *Geophysical Research Letters*, *43*, 4026–4032. https://doi.org/10.1002/2016GL068509

Westra, S., Fowler, H. J., Evans, J. P., Alexander, L. V., Berg, P., Johnson, F., et al. (2014). Future changes to the intensity and frequency of short-duration extreme precipitation. *Reviews of Geophysics*, *52*, 522–555. https://doi.org/10.1002/2014RG000464

Xie, P., Joyce, R., Wu, S., Yoo, S.-H., Yarosh, Y., Sun, F., & Lin, R. (2017). Reprocessed, bias-corrected CMORPH global high-resolution precipitation estimates from 1998. *Journal of Hydrometeorology*, *18*(6), 1617–1641. https://doi.org/10.1175/JHM-D-16-0168.1